FORMABILITY OF AUSTENITIC STAINLESS STEEL 316 SHEET IN DYNAMIC STRAIN AGING REGIME

Syed Mujahed Hussaini[1)], Swadesh Kumar Singh[2)*], Amit Kumar Gupta[1)]
[1)]Mechanical Engineering Department, BITS-Pilani, Hyderabad campus, India
[2)] Mechanical Engineering Department, GRIET, Bachupally, Hyderabad, India

Corresponding author: e-mail:swadeshsingh@griet.ac.in, Tel.:+91(40)64601921, Mechanical Engineering Departmet, GRIET, Bachupally, Hyderabad, 500090, India

Abstract

Dynamic strain aging region for austenitic stainless steel 316 was investigated from room temperature to 650°C at constant strain rates of $1x10^{-2}$, $1x10^{-3}$ and $1x10^{-4}$ sec^{-1}. Characteristics indicators of serrated plastic flow were observed in the temperature range of 400°C to 600°C at these strain rates. Strain rate sensitivity of the material is found to be negative in this region. Study of fracture surface of tensile test specimen by scanning electron microscope revealed that ductility in this region decreased. The limiting drawing ratio of sheet metal is the indicator of formability in deep drawing. LDR of the sheet metal was estimated by performing the deep drawing of different diameter blanks in finite element simulation software LS-DYNA in DSA temperature region. It was observed that in DSA region, formability of sheet metal decreased. These simulations are validated and compared with experimental results.

1 Introduction

Discontinuous plastic flow in metals referred to as dynamic strain aging (DSA). It has been reported and various physical models, micro-mechanisms have been proposed in an attempt to explain this phenomenon [1–2]. The occurrence of DSA during plastic deformation is a well-known phenomenon in metallic materials. It is attributed to the interaction of solute atoms with moving dislocations [3, 4]. It generally observed when the deformation temperature is high enough to permit short range diffusion of solute atoms to dislocation cores. This strong elastic interaction result in a temporary arrest of the dislocation in the slip plane. This DSA always appears during the plastic deformation process of metallic materials under certain temperatures and strain rates. It was found in recent years that the influence of DSA phenomenon on the mechanical behavior of materials should not be ignored [5–7]. Most of the literature shows that the tensile strength [8, 9] and fatigue strength [10, 11] of the material are increased by DSA and ductility and rupture toughness [12] are also influenced.

Typical macroscopic features of DSA include serrated flow behavior, sharp yield points, maxima in the work hardening temperature plot, negative strain-rate sensitivity. Both interstitial and substitutional elements are the responsible for such effects in an appropriate range of strain-rate and temperature. Mobile dislocations move by successive jerks between 'forest' obstacles, i.e. other dislocations piercing their slip plane. Solute atoms diffuse to and age mobile dislocations while they are temporarily arrested at these obstacles. This mechanism leads to

negative strain rate sensitivity (SRS) of the flow stress in a range of strain rates where the two types of defects have comparable mobility [13, 14]. No material particle deforms at a plastic strain rate from within this interval. If the imposed strain rate falls into this range, plastic flow is heterogeneous, with plastic strain rate highly localized in narrow bands, either static or propagating in a continuous or discontinuous manner.

Austenitic stainless steels are particularly suited to the study of DSA mechanisms because of the large temperature range over which serrated flow can occur [15, 16]. Certain solute atom concentrations and at some specific strain rates over which serrated flow may be observed [17, 18]. The temperature range for serrated flow indicates a thermally activated behavior. Tensile tests of an AISI310 type austenitic stainless steel have shown [19] that serrated yielding is observed within a certain range of strain rates and temperatures, where the dynamic strain hardening is high. Both the activation volume and the activation energy for plastic deformation are a function of temperature, and increase with an increase in test temperature. The austenitic stainless steel as the structural components in petrochemical industry, power plants and nuclear reactors is usually served under a load with long period of time at a high temperature region, and it is influenced by DSA during deformation.

The present work tried to study the DSA phenomenon in austenitic stainless steel 316. The serrated flow behavior of the material is one of the evident features of DSA phenomenon and also this region is characterized by negative strain rate sensitivity. The temperature range and strain rate where serrations can observed in flow stress diagram were investigated. The strain rate sensitivity index which is evident of DSA was characterized in this range. This non-classic mechanism takes place at higher temperatures and causes more drastic changes in ductility. Nature of fracture of the tensile specimens was analyzed by Scanning electron microscope (SEM).

Deep drawing is one of the important but very complex forming process where the sheet metal blank is subjected to the different types of stresses. The limiting drawing ratio (LDR) is commonly used to measure the formability of sheet metal in deep drawing. The LDR is defined as the ratio of the maximum blank diameter to the cup diameter which can produce in a single stroke without fracture. In this study the deep drawing simulations were performed in the explicit finite element code LS-Dyna on the different diameter blanks and found the LDR of ASS 316 sheets in and below the DSA region. Effect of DSA on the formability was analyzed.

2 Experimental material and methods

Material used in this study is ASS 316 sheet of 1.0 mm thick. Chemical composition of ASS316 sheet metal blank is listed in **Table 1**. This alloy contains 2.42% molybdenum which enhances the corrosion resistance. This steel is more resistant to general corrosion, pitting and crevice corrosion than the conventional chromium-nickel austenitic stainless steels such as Alloy 304. Resistance to corrosion in the presence of chloride or other halide ions is enhanced by higher chromium (Cr) and molybdenum (Mo) content. This alloy also offers higher creep, stress-to-rupture and tensile strength at elevated temperatures. It is primarily austenitic phase and small quantities of ferrite may be present. Due to the presence of these phases it has excellent toughness besides high strength. These combinations of properties provide the excellent formability to the material.

Table 1 Chemical composition of ASS 316

Element	Fe	Cr	Ni	Mo	Si	Mn	Cu	Co	C
Composition (Wt. %)	67.69	16.63	10.85	2.42	1.28	0.38	0.21	0.21	0.018

Tensile testing was conducted on Universal testing machine (UTM) made by MCS. It is electronic screw driven machines with precision screw, column construction and completely controlled by computer. It has variable speed drive. For conducting test at higher temperature, this machine is attached with a special type split furnace. It is having uniform distribution of heating coils, which are arranged in three zones to achieve temperature up to 1200° C with ± 1°C accuracy. Temperature control and measurement is done by thermocouple. Tests were conducted in air by maintaining constant strain rate of $1x10^{-2}$, $1x10^{-3}$ and $1x10^{-4}$ sec^{-1} in the temperature region from 50 to 650°C. Flat tensile specimen blanks were cut from the flat sheets. The tensile specimens having 30 mm gauge length and 6.4 mm gauge width according to ASTM standard E8M (Sheet type sub-size specimen) were cut from the blanks. Tensile properties were evaluated and draw the true stress and true strain diagram to find the temperature range where the serration occurs, which is characterized as DSA. The fracture surfaces of tensile failed specimens were examined by scanning electron microscope to study the nature of fracture in DSA region.

The deep drawing experiments were carried out on the experimental test rig. This test rig is specially designed for deep drawing operations which can be performed at elevated temperatures. Complete punch and die setup is made with Inconel-600 to prevent the materials to change dimensions at higher temperatures. An induction furnace was developed to heat the blank to maximum temperature of 400°C. Two sets of furnaces were installed on a 20 ton hydraulic press. One furnace is utilized to heat the blank and another is attached to the lower die in order to prevent the blank from becoming cold before actual drawing starts. A continuous coolant supply is provided for the heaters of the die and blank to prevent overheating. The temperatures are recorded by using pyrometer which is a non-contact temperature detecting instrument. This works on the principle of capturing the wavelength of the radiation that is emitted by the material. A data acquisition system which is connected to the press obtains input parameters like punch travel, load applied on the blank, blank holding pressure during deep drawing. These are fed to the computer where it directly plots outputs like variation of load with displacement and blank holding pressure.

3   Finite element simulation

Finite element methods have been extensively used in forming operations to optimize various process variables in order to produce defect free parts. The input models like die, blank, blank holder and punch were constructed in pre-processor dynaform. After the surface was created, fine meshing was generated on the surface of the tool components and the blank. This gives automatically the nodes. Fine meshing is done on the blank to obtain accurate results. The complete tooling model of the pre-processor is shown in **Fig. 1**.

The blank and the tool components were meshed using Belytschko- Tsay shell elements as it takes less computational time, around 30–50% less than others [20]. Material properties were measured at different temperatures with the universal testing machine (UTM) which is coupled with the furnace and given as input to Dynaform to run the simulation. Friction in deep drawing under warm conditions can be reduced by using molycote as lubricant, which is calculated by

Singh et al [21] at various temperatures. Simulations were repeatedly performed by changing the size of the blank and keeping the other parameters constant. The blank holding force and punch speed were similar to those used in the experiments.

Barlat's yield criteria are chosen as the material model in simulations. This criteria incorporates the effect of both normal and planar anisotropy in the yielding behavior of the material. This model was developed by Borliate and Lian [22] for modeling the sheets with anisotropic materials under plain strain conditions. This material model allows use of Lankford parameter in 0°, 45° and 90° to the rolling direction for the defining of anisotropy. Anisotropic yield criterion for plane stress is defined in equation (1). The anisotropic material constants a, c, h and p are obtain through Lankford parameters [22].
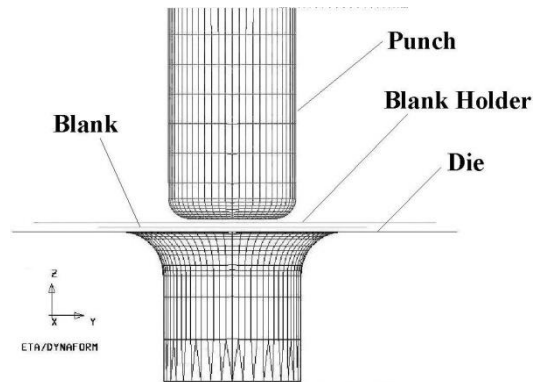
Fig.1 Construction of tooling in pre-processor

$$\phi = a|K_1 + K_2 \; |^m + a|K_1 - K_2 \; |^m + c|2k_2 \; |^m = 2\sigma_Y{}^m \tag{1}$$

Where σ_y is the yield stress and K_i are given by

$$K_1 = \frac{\sigma_x + h\sigma_y}{2} \tag{2}$$

and

$$K_2 = \sqrt{\frac{\sigma_x - h\sigma_y}{2}} + P^2\tau_{xy} \tag{3}$$

4 Results and discussion

4.1 The DSA phenomenon

After conducting the tensile test as per ASTM standard true stress vs true strain graphs are constructed to find the serration. Serrations in the stress–strain curve were observed at lower strain rates. For the entire set of tests, serrations were observed only over a limited range of strain-rate and temperature, as summarized in **Table 2**.

DSA serrations on the stress–strain curves are well-defined at the testing of lower strain rate and temperatures of 400°C to 600°C, while at the lower temperature they are absent in the whole range of the strain rates. **Fig. 2** provides a graphical summary of the results of tensile test carried at lower strain rate 1×10^{-4} sec^{-1}. It is clearly seen that the serrated flow appears at certain temperature at this strain rate.

**Table 2** Serration in flow stress curve for ASS 316 at different strain rate and temperatures

Strain Rate	Temperature (°C)												
	50	100	150	200	250	300	350	400	450	500	550	600	650
10^{-2}	X	X	X	X	X	X	X	X	✓	✓	✓	✓	X
10^{-3}	X	X	X	X	X	X	X	✓	✓	✓	✓	✓	X
10^{-4}	X	X	X	X	X	X	X	✓	✓	✓	✓	✓	X
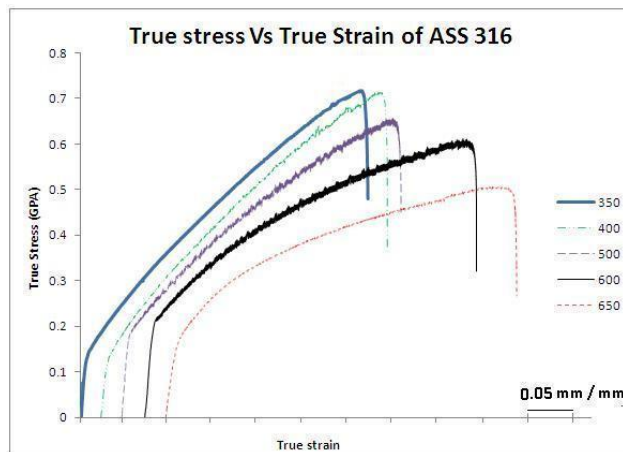
Fig.2 Flow stress curve of ASS316 at constant strain rate of 1×10^{-4} sec^{-1}

The strain-rate sensitivity index (m) is considered to be the one of the parameter that can characterize DSA phenomena. The flow stress equation that describes plastic behavior is usually written as equation (4) where 'σ' is the flow stress, 'K' is a material constant, '$\dot{\varepsilon}$' is the strain rate and 'm' is the strain-rate sensitivity index of the flow stress. The m-value is a function of the forming parameters, such as the strain rate and the temperature. The most convenient method of measuring 'm' is a uniaxial tensile test at a particular constant temperature and at different strain rates. The simplest method is reflected in the relationship between the flow stress (σ) and the strain rate ($\dot{\varepsilon}$).

$$\sigma = K\dot{\varepsilon}^{m} \tag{4}$$

The 'm' value is usually calculated from the logarithmic plot of the flow stress vs strain rate. **Fig. 3** shows the graph at DSA temperature range covering the true strains of 0.2. The 'm' values were calculated from the slopes of the graph. The negative value of 'm' for the temperature from 400°C to 600°C evident the occurrence of DSA. Decreasing strain rate sensitivity with increasing strain in the DSA regime has been reported in low carbon steel [23] and subsequently analyzed in detail by McCormick [24]. The appearance of negative strain-rate sensitivity coincides with the appearance of serrations in the stress–strain curves, again suggesting solute induced dynamic strain aging.
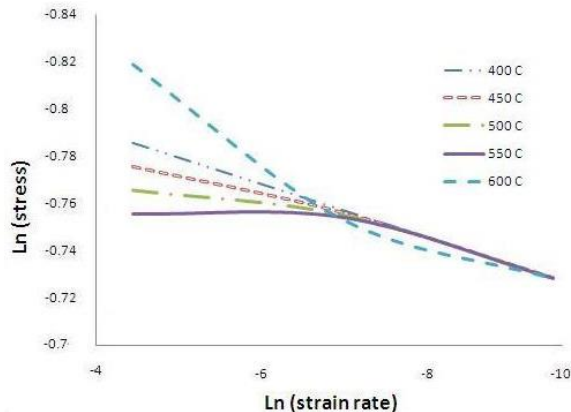
Fig.3 True stress Vs True strain rate graph on log scale

The occurrence of the serration is linked to a bounded region of negative strain-rate dependence of the flow stress, which may be explained by DSA resulting from diffusion of solute atoms to dislocations temporarily arrested at obstacles in the slip path [27]. It clearly indicates that within the temperature range where serrated flow occurs, the strain rate sensitivity of the flow stress becomes negative. This serrated flow to originate from the pinning of dislocations by solute atoms of the alloy. These are attributing the occurrence of DSA in ASS 316.
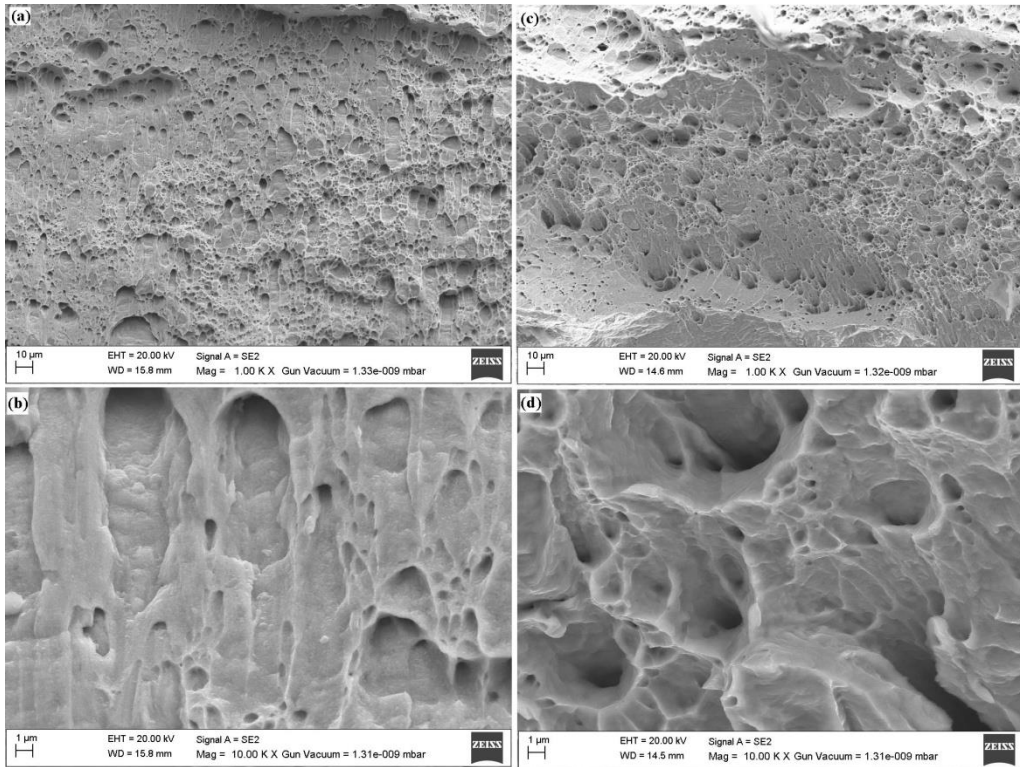
4.2 Fracture study

SEM photographs of the fracture surface of tensile specimens at 300°C and 550°C are shown in **Fig. 4** at different magnifications. There is a difference in the fracture surface. Fracture usually occurs under single load or tearing. This is shown by depressions in the microstructure called dimples, which occur from micro void emergence in places of high local plastic deformation. The observed micro voids can be generated from non-metallic inclusions. For example, voids on the surface may be initiated by carbide inclusions or nucleates at precipitates. At 300°C, the large dimples developed at non-metallic inclusions can be seen. Under increased strain, micro voids grow, coalescence, until rupture occurs, thus dimples fracture. Dimple size and shape depends on the type of loading and extent of micro void emergence. When a material is put under uniaxial tensile loading, equi-axed dimples appear which have complete rims. Under a shear loading the dimples are elongated, the rims of the dimples are not complete and the dimples are in the same direction as the loading. Oval dimples occur when a large void intersects a smaller subsurface void the dimples form an oval shape and exhibit complete rims.

Fracture surface at 550°C consists of small dimples and flat areas looking like semi-cleavage. The flat area of fracture occurs without significant plastic deformation. These are also looking like quasi cleavages. Cleavage results from high stress along three axes with a high rate of deformation. Characteristics of cleavage are cleavage steps, feather markings, herringbone structure, tongues and micro-twins, Wallner lines and quasi-cleavage. A cleavage step is a step on a cleavage facet joining two parallel cleavage fractures. Feather markings are very fine, fan like markings on a cleavage fracture. Quasi cleavage is a fracture mode resembling cleavage because of its planar facets but where the fracture facets are not specific well-defined planes.

This difference of fracture surface is in agreement with variation of nature of fracture at these conditions. At non DSA region of 300°C fracture occurred through severe plastic deformation

results in large dimples which show that fracture is ductile. Whereas in DSA region at 550°C fractured surface had small dimples and quasi-cleavage which shows fracture is less ductile. With this it can be observed that in DSA region ductility of the material decreases.

Fig.4 SEM images of fracture surface of 300°C and 550°C (a) 1000X at 550°C (b) 10, 000X at 550°C (c) 1000X at 300°C (d) 10, 000X at 300°C

4.3 Formability study

**Fig. 5** shows the drawn cup from the blanks of 74 mm diameter by LS Dyna at 300°C
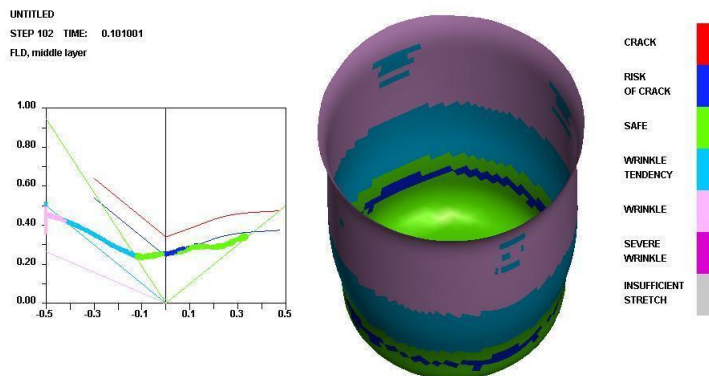
Fig.5 Drawn cup at 300°C from ø74 mm blank and FLD by FEM

temperature and forming limit diagram (FLD) of the cup. FLD is a graph between the minor strain and major strain of the sheet metal. Possibility of fracture in cup can analyze and compared with the forming limit curve (FLC), which appears in FLD. It shows that strain in the cup is below FLC and drawing is in the safe zone. There is no indication of fracture in the cup walls. Thickness of the cup at punch corner is reduced to 0.88 mm without necking. At this temperature when 75 mm blank was drawn, the strain in the cup crosses the FLC as shown in **Fig. 6**, which is not safe. The thickness at punch corner is reduced to less than 0.2 mm which indicates the fracture. Fracture occurred at the punch corner due to excessive strain. At 300°C temperature maximum of 74 mm diameter blank can draw into 30 mm cup without fracture hence LDR is 2.47.
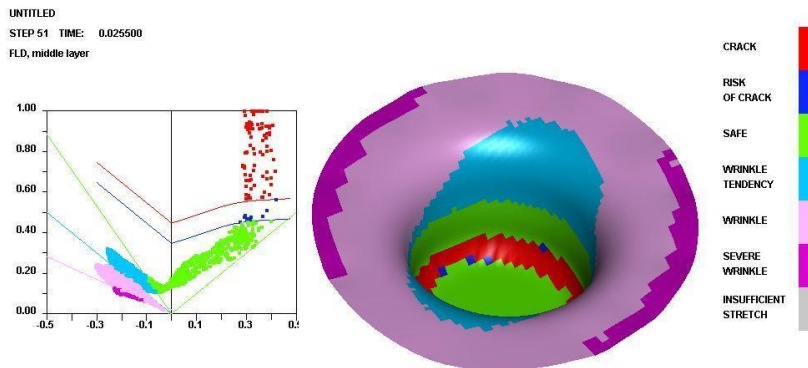
Fig.6 Fracture in the cup drawn from ø75 mm blank and FLD at 300°C

Finite element simulations were performed on the blank of same diameter but at higher temperature of 400°C. As the temperature increases, these higher sizes of the blanks can be deep drawn safely but here it fractured in the cup. At this temperature maximum of 72 mm diameter blank can be deep draw safely as shown in **Fig. 7**.
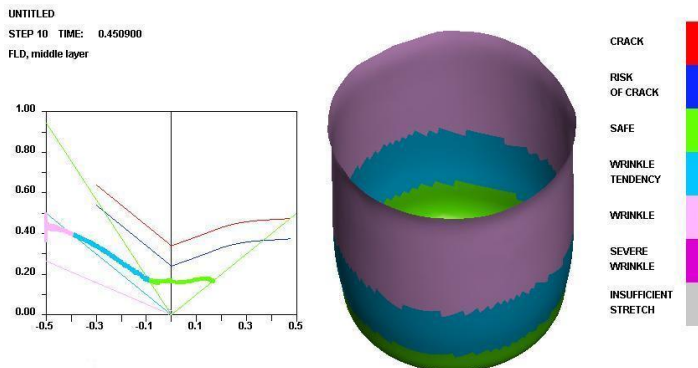
Fig.7 Deep drawn cup from ø72 mm blank at 400°C

This temperature is in the DSA region which makes the blank to fracture during deep drawing. It leads to fracture at punch corner. In the DSA region LDR is reduced. At the elevated temperatures, cups are drawn from the higher size of the blanks without fracture but here due to

occurrence of DSA, LDR decreased. It shows that in the DSA region formability of the sheet metal decreased. Experimentally drawn cups from 72 mm, 74 mm and 76 mm diameter blanks at 300°C temperature are shown in **Fig. 8**.

Maximum of 74 mm blanks are drawn into cups at this temperature. Next higher size of the blank of 76 mm fractured at punch corner. So the limiting drawing ratio at this temperature is 2.47. These experiments confirm the FE predictions.

Fig.8 Experimentally drawn cups at 300°C

Fig. 9 shown the cups drawn from the same size of the blanks but at higher temperature 400°C. Here the cups are drawn only from 72 mm blank whereas 74 mm blank fractured during drawing. LDR of the material is decreased to 2.4. But from the previous work it was investigated that as the temperature increased, LDR of sheet metal increases [25]. At the temperature of 400°C, ASS 316 has undergone DSA phenomena. During DSA phenomena temporary arrest of the dislocation in the slip plane due to the interaction of solute atoms with moving dislocations in the material, which results in the increase of the strength of the sheet. During this phase as the force to draw the cup gradually increased. Once the dislocation escaped from the solute atoms, the strength of the material decreased but punch force has remained higher, which leads to localize fracture initiations in the material. This makes the sheet material fractured before complete forming which leads to brittle fracture. At the higher size of the blank, force to draw the cup is higher and this force for 74 mm blanks fractured the cup before complete drawing. Limiting drawing ratio of ASS 316 decreased in DSA region. This shows that formability of this material decrease in DSA region.
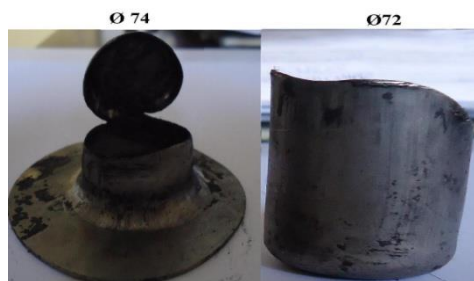
Fig.9 Experimentally drawn cups at 400°C

5   Conclusions

In this study, DSA region of austenitic stainless steel 316 had been investigated by uniaxial tensile test. Occurrence of serrated plastic flow and negative strain rate sensitivity of the flow stress curve indicate the presence of DSA in the temperature range of 400°C to 600°C. Forming of quasi cleavages on the fractured surface of the tensile test specimen in the DSA region were

observed. In the DSA region ductility of the material decreased. Deep drawing of the sheet blanks were simulated in LS Dyna and measure the LDR below and in DSA region. In the DSA region LDR was decreased and it concluded that the formability of sheet metal decreased in the DSA region. Simulations were in good agreement with the experimental results.

References

[1] Z. Kovacs, J. Lendvai, G. Voros: Material Science and Engineering A, Vol. 279, 2000, p. 179-184, DOI:10.1016/S0921-5093(99)00628-0

[2] A.K. Gupta, V.K. Anirudh, S.K. Singh: Materials and Design, Vol. 43, 2013, p. 410-418, DOI: 10.1016/j.matdes.2012.07.008

[3] M.A. Soare, W.A. Curtin: Acta Materialia, Vol. 56, 2008, p. 4091-4101, DOI: 10.1016/j.actamat.2008.04.030

[4] P. G. McCormick: Acta Metallurgica, Vol. 36, 1988, p. 3061-3067, DOI: 10.1016/0001-6160(88)90043-0

[5] S.K. Singh, A.K. Gupta, K. Mahesh: Materials and Design, Vol. 31, 2010, p. 2288-2295, DOI: 10.1016/j.matdes.2009.12.012

[6]   F. Chmelik, A. Ziegenbein, H. Neuhauser, P. Lukac: Materials Science and Engineering A, Vol. 324, 2002, p. 200-207, DOI: 10.1016/S0921-5093(01)01312-0

[7] S. Herenu, I. Alvarez-Armas, A.F. Armas: Scripta Materialia, Vol. 45, 2001, p. 739-745, DOI: 10.1016/S1359-6462(01)01088-0

[8] A.K. Gupta, S.K. Singh, M. Swathi, H. Gokul: Materials and Design, Vol. 35, 2012, p. 589-595, DOI: 10.1016/j.matdes.2011.09.060

[9] D. Wagner, J.C. Moreno, C. Prioul: Journal of Nuclear Materials, Vol. 252, 1998, p. 257-265, DOI: 10.1016/S0022-3115(97)00279-1

[10] M.G. Moscato, M. Avalos, I. Alvarez-Armas, C. Petersen, A.F. Armas: Materials Science and Engineering A, Vol. 234–236, 1997, p. 834-837, DOI: 10.1016/S0921-5093(97)00405-X

[11] K.W. Lee, S.K. Kim, S.I. Hong, Journal of Nuclear Materials, Vol. 295, 2001, p. 21-26, DOI: 10.1016/S0022-3115(01)00509-8

[12] C.S. Seok, K.L. Murty: International Journal of Pressure Vessels and Piping, Vol. 76, 1999, p. 945-953, DOI: 10.1016/S0308-0161(99)00075-7

[13] A. Benallal, T. Berstad, T. Borvik, A.H. Clausen, O.S. Hopperstad: European Journal of Mechanics - A, Vol. 25, 2006, p. 397-424, DOI: 10.1016/j.euromechsol.2005.10.007

[14] Kil Soo Kim, Robert L. Piziali: International Journal of Solids and Structures, Vol. 23, 1987, p. 1563-1578, DOI: 10.1016/0020-7683(87)90070-9

[15] M. Ivanchenko, Y. Yagodzinskyy, H. Hänninen: Materials Science and Engineering: A, Vol. 521–522, 2009, p. 121-123, DOI: 10.1016/j.msea.2008.09.093

[16] C. Gupta, J.K. Chakravartty, S.L. Wadekar, J.S. Dubey: Materials Science and Engineering A, Vol. 292, 2000, p. 49-55, DOI: 10.1016/S0921-5093(00)00992-8

[17] J.K.L. Lai: Materials Science and Engineering, Vol. 58, 1983, p. 195-209, DOI: 10.1016/0025-5416(83)90046-0

[18] L.H. de Almeida, P.R.O. Emygdio, I. Le May: Scripta Metallurgica et Materialia, Vol. 31, 1994, p. 505-510, DOI: 10.1016/0956-716X(94)90134-1

[19] L. Shi, D.O. Northwood: Acta Metallurgica et Materialia, Vol. 43, 1995, p. 453-460, DOI: 10.1016/0956-7151(94)00279-Q

[20] S. S. Kumar, D. R. Kumar: Journal of Materials Processing Technology, Vol. 204, 2008, p. 169-178, DOI: 10.1016/j.jmatprotec.2007.11.060

[21] Swadesh Kumar Singh, M. Swathi, Apurv Kumar, K. Mahesh: Materials and Design, Vol 31, 2010, p. 4478-4484, DOI: 10.1016/j.matdes.2010.04.049

[22] Frédéric Barlat, Daniel J. Lege, John C. Brem, International Journal of Plasticity, Vol. 7, 1991, p. 693-712, DOI: 10.1016/0749-6419(91)90052-Z

[23] P.G McCormick: Scripta Metallurgica, Vol. 12, 1978, p. 197-200, DOI: 10.1016/0036-9748(78)90163-1

[24] P.G. McCormick: Acta Metallurgica, Vol. 36, 1988, p. 3061-3067, DOI: 10.1016/0001-6160(88)90043-0

[25] S. M. Hussaini, S. K. Sing, A. K. Gupta: Journal of King Saud University - Engineering Sciences, In Press, 2013, DOI: 10.1016/j.jksues.2013.05.001